TDMA Versus CSMA/CA for Wireless Multihop Communications: A Stochastic Worst-Case Delay Analysis

Qi Wang, Katia Jaffrès-Runser, *Member, IEEE*, Yongjun Xu, *Member, IEEE*, Jean-Luc Scharbarg, Zhulin An, and Christian Fraboul

***Abstract*—Wireless networks have become a very attractive solution for soft real-time data transport in the industry. For such technologies to carry real-time traffic, reliable bounds on end-to-end communication delays have to be ascertained to warrant a proper system behavior. As for legacy wired embedded and real-time networks, two main wireless multiple access methods can be leveraged: one is time division multiple access (TDMA), which follows a time-triggered paradigm, and the other is carrier sense multiple access with collision avoidance (CSMA/CA), which follows an event-triggered paradigm. This paper proposes an analytical comparison of the time behavior of two representative TDMA and CSMA/CA protocols in terms of the worst-case end-to-end delay. This worst-case delay is expressed in a probabilistic manner because our analytical framework captures the versatility of the wireless medium. Analytical delay bounds are obtained from delay distributions, which are compared to fine-grained simulation results. Exhibited study cases show that TDMA can offer smaller or larger worst-case bounds than CSMA/CA depending on its settings.**

***Index Terms*—CSMA/CA, IEEE802.11 DCF, stochastic worst-case end-to-end delay, time division multiple access (TDMA), wireless multihop networks.**

I. Introduction

WIRELESS multihop networks (i.e., ad hoc, sensor, and mesh networks) are currently being intensively investigated for real-time applications because of their appealing ease of deployment and scalability [1], [2]. Many industrial applications require delay guarantees in their networks: Packets of critical flows must arrive at their destination within a fixed delay bound. Guaranteeing hard real-time communications in wireless networks is difficult due to the unreliability of the wireless channel. However, it is possible to guarantee soft real-time requirements with a dedicated protocol stack design. Such networks can tolerate a really small probability for the end-to-end delay of flows to exceed a fixed time limit. In these networks, it is thus possible to derive a probabilistic worst-case delay bound d^w with a given confidence level.

As for legacy wired embedded and real-time networks, two main types of multiple access methods can be leveraged: 1) time division multiple access (TDMA), which follows a time-triggered paradigm, and 2) carrier sense multiple access with collision avoidance (CSMA/CA), which follows an event-triggered paradigm. So far, wireless real-time networking solutions rely on a mesh topology where TDMA is exploited for its high determinism [2]. CSMA/CA is the solution chosen for mainstream nontime-sensitive wireless networking for its scalability and elastic bandwidth management capability.

Several studies have looked at the benefits of CSMA/CA solutions for soft real-time networking and compared their performance to TDMA solutions. Most of these works have evaluated both approaches using simulations and experiments. In this paper, we propose to look at the problem from a theoretical point of view. There is still a need for a comprehensive analytical framework capable of calculating the worst-case delay bounds of flows carried on a given wireless network [3]. The problem is not easy since wireless communications have to be modeled with a link transmission probability. Modeling the multihop, multiflow interactions requires advanced performance evaluation models (e.g., Markov chain, Z-transforms, etc.) whose assumptions are not always realistic.

This paper introduces a new method to calculate the delay distribution of a basic TDMA protocol. It relies on an analytical framework that we have previously defined to capture the performance (in average) of multihop multiflow wireless networks [4]. From this delay distribution calculation, we can derive the stochastic worst-case delay bound of TDMA for any topology and flow pattern. This delay distribution and the worst-case bound are validated against extensive simulations. Next, we leverage this new TDMA bound calculation to compare the performance of TDMA to the one of CSMA/CA on two elementary network topologies. Therefore, the analytical model of [5] we had validated for CSMA/CA is applied to the

This work was supported in part by the National Natural Science Foundation of China under Grant 61602447 and Grant 61303245. Paper no. TII-16-0461.R1. *(Corresponding author: K. Jaffrès-Runser.)*

Q. Wang, Y. Xu, and Z. An are with the Institute of Computing Technology, Chinese Academy of Sciences, Beijing 100864, China (e-mail: wangqi08@ict.ac.cn; xyj@ict.ac.cn; anzhulin@ict.ac.cn).

K. Jaffrès-Runser, J.-L. Scharbarg, and C. Fraboul are with the Institut de Recherche en Informatique de Toulouse, Université de Toulouse, INPT, Toulouse F-31061, France (e-mail: kjr@enseeiht.fr; jean-luc.scharbarg@enseeiht.fr; christian.fraboul@enseeiht.fr).

Digital Object Identifier 10.1109/TII.2016.2620121

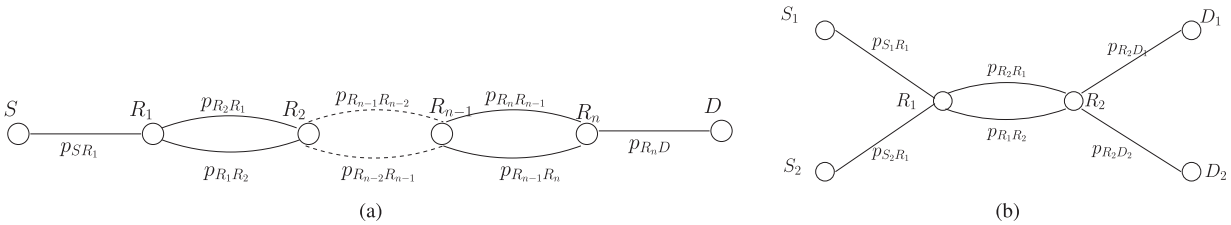

Fig. 1. Investigated topologies: (a) linear topology composed of one flow and x relay nodes; and (b) cross flow topology where two flows share a specific path composed of two relay nodes.

selected topologies. Several TDMA configurations are tested. As expected, TDMA can be made more or less efficient than CSMA/CA depending on its settings. It is interesting to note that our model clearly captures the longer tail of the delay distribution of CSMA/CA compared to TDMA.

This paper is organized as follows. Section II introduces network models and protocols related to both multiple access schemes. Section III pictures the main elements of the analytical models proposed herein for the end-to-end delay distribution computations of TDMA and CSMA/CA. Section IV validates our analytical models against simulations. Following, it compares the performance of TDMA and CSMA/CA on two topologies. Section V identifies main related works, and finally, Section VI concludes this paper.

II. System Model and Protocols

A. Multihop Topologies

In this paper, we investigate two different atomic topologies that are at the core of many deployment scenarios of wireless multihop communications. First, we will concentrate on a linear deployment scenario, as shown in Fig. 1(a). Such scenarios are typical where coverage needs to be extended in a specific direction. Linear topologies are for instance deployed to extend coverage on demand using swarms of drones over a stadium [6]. The second 2-relay/2-flow topology has been investigated to capture the contention effect of a set of nodes carrying multiple flows.

The linear topology is a basic multihop topology, where all packets are forwarded from one source node S to a destination node D using relay nodes. In our case, we choose a topology where x nodes relay the frames from S to D [cf., Fig. 1(a)]. In Section IV, we will provide results for x equal to 3, 4, or 5. The more relays are exploited, the higher the odds for the transmission to fail. Typically, end-to-end communications exceeding four to five hops get more difficult to implement in practice. The second topology investigated is the 2-relay/2-flow topology of Fig. 1(b). Here, the two relays have to forward packets that belong to two flows, simultaneously. The first flow is emitted by S_1 going to D_1 and the second flow is emitted by S_2, going to D_2. This situation is critical since the relays have to listen to both flows and to re-emit them concurrently.

Source nodes generate strictly periodic flows of frames. As we will explain later in Section IV, we set the frame generation period such as there is only one frame in the emission buffer of the source at all times. Thus, the only delay we are computing analytically or measuring by simulation is the MAC delay, i.e., the time for the frame to gain access to the channel. There is no delay related to queuing in this work.

Algorithm 1: TDMA Scheduling of Node j in Time Slot u.

```
if memory of slot u not empty then
    Send the packet;
else
    if node j receives a packet p from i in slot u then
        Generate a random value x ∈ [0, 1];
        for each time slot v ∈ T, v ≠ u do
            if v==1 and x ≤ x_ij^u1 then
                Store the packet p into memory of slot 1;
            else
                if x_ij^u(v−1) ≤ x ≤ x_ij^uv then
                    Store the packet p into memory of slot v;
                end if
            end if
        end for
    end if
end if
```

B. CSMA/CA Network Model and Protocol

We assume in this work that all nodes of the network follow the state-of-the-art IEEE802.11 DCF MAC protocol. We refer the reader to the IEEE802.11-2012 norm for a detailed description of the IEEE802.11 DCF MAC protocol and to [5] for a primer on the subject. The DCF mechanism can be extended by the RTS/CTS message exchange to avoid the hidden terminal problem. In this case, before initiating a communication, the emitter sends a Request To Send (RTS) frame. The destination node then emits a Clear To Send (CTS) frame to notify nodes that have not received the initial RTS of the imminent transmission start. The CSMA/CA protocol is completely distributed and thus can be very easily deployed.

C. TDMA Network Model and Protocol

A perfectly synchronized TDMA is considered. A superframe of $|T|$ time slots is repeated indefinitely. For the 2-relay/2-flow scenario, $|T| = 4$. The source S_1 emits its frames in time slot 1, source S_2 in slot 2, relay R_1 in slot 3, and relay R_2 in slot 4. Similarly, for the 3-relay scenario, $|T| = 4$ with the source emitting in time slot 1, and relays R_i in time slot number $i + 1$. As shown in Fig. 1, there are bidirectional links between relays but not between sources and relays, nor between relays and destinations. It is a way to represent multiple paths, by allowing circular paths with different lengths.

In our TDMA network model [4], each relay node is characterized by a set of uniform *forwarding probabilities* x_{ij}^{uv} that govern its forwarding decisions. Assuming node j receives a

TABLE I
FORWARDING PROBABILITIES AND EMISSION RATES FOR 2-RELAY AND 3-RELAY SCENARIO SETTING IN TDMA

	$x^{13}_{S_1R_1}$	$x^{14}_{S_1R_2}$	$x^{23}_{S_2R_1}$	$x^{24}_{S_2R_2}$	$x^{34}_{R_1R_2}$	$x^{43}_{R_2R_1}$	$\tau^1_{S_1}$	$\tau^2_{S_2}$	$\tau^3_{R_1}$	$\tau^4_{R_2}$
2-flow 2-relay scenario										
Unique Solution	0.49	0	0.49	0	0.95	0.02	1	1	0.9986	0.9487

	$x^{12}_{SR_1}$	$x^{13}_{SR_2}$	$x^{14}_{SR_3}$	$x^{23}_{R_1R_2}$	$x^{24}_{R_1R_3}$	$x^{32}_{R_2R_1}$	$x^{34}_{R_2R_3}$	$x^{42}_{R_3R_1}$	$x^{43}_{R_3R_2}$	τ^1_S	$\tau^2_{R_1}$	$\tau^3_{R_2}$	$\tau^4_{R_3}$
1-flow 3-relay scenario													
$S_{\min}$	0.94	0	0	0.95	0	0	0.95	0	0.11	1	0.94	0.997	0.947
S_{middle}	0.58	0	0	0.95	0	0	0.95	0	0.47	1	0.58	0.995	0.9945
$S_{\max}$	0.12	0	0	0.85	0	0	0.95	0	0.94	1	0.12	0.9524	0.9048

packet from node i in the current superframe s in time slot u, it decides on the next emission slot v following Algorithm 1. As such, a packet may travel one hop in the duration of *at most* one superframe. The forwarding probability $x^{\mathrm{uv}}_{\mathrm{ij}}$ is the probability to forward the packet received from node i in slot u of super frame s in the time slot v of next superframe $s+1$. Node j only re-emits at most once a packet received in slot u as $\sum_v x^{\mathrm{uv}}_{\mathrm{ij}} \leq 1$. In case $\sum_v x^{\mathrm{uv}}_{\mathrm{ij}} < 1$, the packet may be dropped with probability $1 - \sum_v x^{\mathrm{uv}}_{\mathrm{ij}}$.

Each node of the network is represented by its emission rate in a slot. The emission rate τ^u_i represents the proportion of time a node i is active in a slot u, in average. For instance, a value of $\tau^u_i = 0.5$ means that node i is emitting in slot u in every two superframes. Source nodes have an emission rate of 1 in time slot 1 for both topologies.

To ensure flow conservation and capture the cross-layer effect, the relay nodes have an emission rate that is proportional to the amount of packets they receive from other nodes and their respective forwarding probabilities. The amount of packets they receive is a function of the number of packets other nodes have sent, and the link quality over which they have been received. The link quality is quantified by a channel probability p^u_{ij} that represents the chances for a packet to be properly received in time slot u over link (i,j). This channel probability is derived from the average packet error rate on link (i,j) and from the emission rates of sending nodes. (cf., [4] for details). Flow conservation is ensured if the following set of $|E|$ equations is ensured:

$$\sum_{(i,j)\in\overrightarrow{\mathcal{N}^u_j}} \sum_{u\in\mathcal{T}} \tau^u_i p^u_{\mathrm{ij}} x^{\mathrm{uv}}_{\mathrm{ij}} = \tau^v_j \quad \forall (j,v) \in E \tag{1}$$

where $\tau^u_i p^u_{\mathrm{ij}}$ is the probability that a packet sent by i in time slot u arrives in j. $|E|$ is given by the number of edges times the number of slots. $\overrightarrow{\mathcal{N}^v_j}$ is the set of outgoing edges coming into node j from any node i in time slot u.

Based on this TDMA network model, we have shown in [4] that it is possible to calculate, for a given matrix of forwarding probabilities X, various performance metrics using a steady-state computation reminiscent of a Markov chain. The two main performance metrics we have defined are the so-called *capacity-achieving average end-to-end delay* f^c_D and *capacity-achieving average energy* f^c_E metrics. Both are to be minimized and are, respectively, equal to the average end-to-end delay f_D and the average energy consumed f_E normalized by the throughput f_C

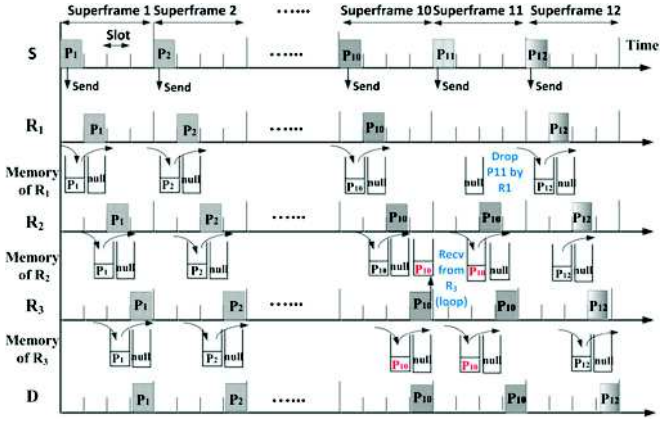

Fig. 2. Example of our TDMA protocol (1-flow 3-relay networks with solution $S_{\min}$ given in Table I). P_1, P_2 experience a direct path to the destination. P_{10} uses the loop between R_3 and R_2, while R_1 drops P_{11} due to flow conservation constraint.

defined in [4]. As such, we have the relations: $f^c_D = f_D/f_C$ and $f^c_E = f_E/f_C$. Since both f^c_D and f^c_E metrics are normalized by the achieved capacity f_C, each solution's performance is scaled to the actual throughput the whole system offers. As such, these metrics measure how much delay and how much energy it would cost to push all data through the system (they are capacity-achieving). In terms of units, f^c_D is expressed in number of hops as it gives the average number of hops required for a packet to arrive in D. For f^c_E, it represents the number of Joules required by all emissions and reception operations for one packet to arrive at its destination.

For the two topologies investigated in this work, we have calculated the Pareto-optimal forwarding probabilities given in Table I. These forwarding probabilities have been derived using a multiobjective optimization problem formulation where capacity-achieving delay (f^c_D) and capacity-achieving energy (f^c_E) are minimized concurrently (cf., [4] for a detailed definition). The solutions provide the best tradeoffs between these two performance metrics. The multiobjective problem has been solved with the NSGA-2 algorithm. In our multiobjective problem, we have to add the constraint $x_{R_{(i)}R_{(i-1)}} \leq 1-\Delta$ and $x_{R_{(i-1)}R_i} \leq 1-\Delta$ ($\Delta = 0.05$) to ensure convergence of the Markov model to steady state (cf., [4]).

For the 2-relay scenario, only one solution is tested because the whole search has resumed to a single Pareto-optimal point, as represented in Fig. 3(a). For the 3-relay scenario, three

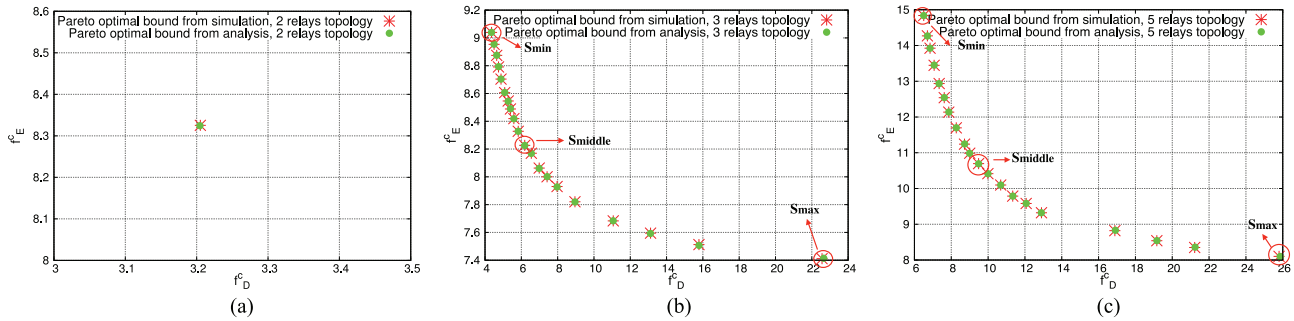

Fig. 3. Capacity-achieving Pareto optimal bounds for TDMA network. *x*-axis (respectively *y*-axis) represents the average duration in milliseconds (respectively in Joules) for one packet received at the destination. (a) Pareto optimal bound for 2-relay wireless networks, (b) Pareto optimal bound for 3-relay wireless networks, and (c) Pareto optimal bound for 5-relay wireless networks.

forwarding solutions are investigated further in this work, all extracted from the Pareto-optimal set of Fig. 3(b). The first one, $S_{\min}$, exhibits the smallest average end-to-end delay (but the highest average energy), the second one, $S_{\max}$, exhibits the largest average end-to-end delay (but the smallest average energy), and the last one, S_{middle}, exhibits an average delay in between smallest and largest. Similar, for the 5-relay scenario, three forwarding solutions are investigated, as shown in Fig. 3(c), respectively.

D. Illustrative Example for TDMA

To clearly understand our TDMA protocol, we picture possible transmission sequences for the 1 flow 3-relay network configured with solution $S_{\min}$ (cf., Table I) in Fig. 2. In this solution, from the forwarding probabilities, a loop exists between R_2 and R_3. In the first two superframes, packets emitted by S are forwarded without using the loop. For instance, P_1 is first re-emitted by relay R_1 in time slot 2, then by R_2 in slot 3, then by R_3 in slot 4 to finally arrive at D. This means that in slot 1, R_1 has received a packet from S and decided following probability $x^{12}_{SR_1} = 0.94$ to store the packet into the buffer of slot 2. In slot 2, R_1 has a packet in its buffer and thus emits it. Still in slot 2, R_2 receives the packet and following probability $x^{23}_{R_1R_2} = 0.95$ chooses to store it in buffer of slot 3. Same steps are repeated in slots 3 and 4.

We also picture other possible (but less likely) sequences with packets P_{10} and P_{11}. Packet P_{10} is received twice because it is overheard by R_2 and sent another time from R_2 to R_3. More specifically, it is forwarded first by R_1 and then by R_2 in the same way than P_1 was. As R_3 receives P_{10}, it decides following $x^{34}_{R_2,R_3} = 0.95$ to emit it in slot 4. Both R_2 and D receive P_{10} (as it happened as well for P_1 and P_2). But this time, R_2 decides to re-emit P_{10} in slot 3 because of $x^{43}_{R_3,R_2} = 0.11$. Thus, R_2 will store P_{10} and emit it in next superframe 11, slot 3. Since flow conservation is enforced by constraint (1), packet p_{11} is dropped by R_1 (this happens with probability $1 - x^{23}_{R_1R_2} = 0.05$).

III. Analytical Delay Distribution and Worst-Case Delay Models

This section introduces the analytical models to derive the delay distributions of both CSMA/CA and TDMA protocols. The probabilistic worst-case end-to-end delay is derived from the delay distribution as defined next.

A. Worst-Case Delay Definition

The delay distribution for a flow ending at destination D_j is given by the *probability mass function* (PMF) and denoted by the probability $P[d_j = d]$, with $d \in \mathbb{R}^+$ being arbitrary positive end-to-end delay values. PMF can be computed for each flow in the network.

The stochastic *worst-case delay* for the flow ending at destination D_j is defined as the delay d^w for which the probability $P[d_j \geq d]$ to find a delay larger than d^w is arbitrarily small (for instance smaller than $\delta = 10^{-9}$). Formally, for a flow ending at D_j

$$d^w = \max\ d \quad \text{s.t.} \quad P[d_j \geq d] \leq \delta. \tag{2}$$

If several flows exist, it is possible to calculate the worst-case delay for all the flows, which is given by the maximum of the d^w values calculated for all possible destinations. Next, we concentrate on the PMF derivation for both CSMA/CA and TDMA schemes.

B. Delay Distribution for CSMA/CA

In our previous work [5], we have analyzed and compared the two main delay distribution derivation methods for the IEEE802.11 DCF protocol proposed in [7] and [8]. Both works elaborate on the discrete time Markov chain model of Bianchi [9]. These Markov chains are derived for a one-hop communication interfered by $n_c - 1$ other nodes that constantly contend for channel access. We refer the reader to [5] to retrieve all mathematical derivations related to our CSMA/CA model. Only main assumptions and necessary derivations are presented next.

As stated earlier, we assume the source generates packets periodically, with a period chosen such as there is one packet arriving in the source buffer when the previous packet has reached its destination. In other words, each packet has time to be flushed through the network before a new end-to-end transmission is attempted. Thus, no frames can build up in the source or relay queues, and there is no queuing delay.

To be able to apply the Markov model of [9], where source and relay nodes compete continuously for the channel (we are at

network saturation), we have to add supplementary interfering nodes. For each single-hop communication, we assume there is a total of $n_c = 3$ nodes contending for channel access simultaneously, including the source of interest. From the derivations given by Vardakas *et al.* [7], we calculate the Probability Generating Function (PGF) of the MAC delay for a one-hop communication. To retrieve the PMF of the single-hop communication, the PGF has to be inverted using the Lattice–Poisson formula given by Vu and Sakurai [10].

To compute the PMF of end-to-end delay in a multihop communication, first, we calculate the PGF of the MAC delay for a one-hop communication. We assume that the delay experienced over one hop is independent of the delay of the other hops. This assumption is reasonable as we are in the saturated scenario, where all emitting nodes constantly contend for the medium. The PGF of the sum of independent random variables is equal to the product of the PGF of each variable. Thus, the analytical PGF of the multihop total delay $d^{\text{multihop}}(Z)$, calculated for any complex number $Z \in \mathbb{C}$, can be derived as the product of the PGFs of MAC delays calculated for each hop, where $\mathbb{C}$ is the set of complex numbers: $d^{\text{multihop}}(Z) = d^1(Z) * d^2(Z) * \ldots * d^h(Z)$, where $d^h(Z)$ is the PGF of the hth hop MAC delay. The value of the PGF $d^h(Z)$ for any complex $Z \in \mathbb{C}$ is given by the Z-transform of the h-th hop MAC delay $d^h[k]$ (a discrete time series where k is an integer): $d^h(Z) = \sum_{k=0}^{\infty} d^h[k] Z^k$. To retrieve the PMF, the numerical Lattice-Poisson inversion method given by Vu and Sakurai [10] is applied with accuracy 10^{-8}.

C. Delay Distribution for our TDMA Protocol

In our model, the delay is measured in hops. A packet may experience several paths, each one of different lengths in number of hops. It takes at most one superframe duration for the packet to travel one hop further. So all metrics of delay are expressed in hops, and can be easily converted in time units by multiplying them by $M \times \varsigma_{\text{slot}}$, where M is the number of time slot and ς_{slot} is the slot duration.

1) Relaying and Arrival Matrix: The relaying matrix Q gives the probabilities for any emission (i, u) in time epoch s (i.e., superframe) to be emitted as (j, v) at the following time epoch $(s + 1)$ by the relays of the networks. The arrival matrix $\mathcal{A}$ is composed of the probabilities to go from any transient state to any absorbing state, i.e., the probabilities for any emission (i, u) at time epoch s to arrive at a destination D_j in time slot v at time epoch $(s + 1)$. N is the number of relays.

The relaying matrix Q is structured as follows:

$$Q = \begin{bmatrix} 0 & Q_{12} & \cdots & Q_{1N} \\ Q_{21} & 0 & \cdots & Q_{2N} \\ \vdots & & & \vdots \\ Q_{N1} & \cdots & Q_{N-1N} & 0 \end{bmatrix}$$

0 is a $|T|$-by-$|T|$ zero matrix representing the fact that a node i never forwards a packet to itself. The matrix Q_{ij} is a $|T|$-by-$|T|$ matrix that gives the probabilities of j to transmit a packet sent by node i for all possible combinations of time slots and is given by

$$Q_{\text{ij}} = \begin{bmatrix} Q_{\text{ij}}^{11} & \cdots & Q_{\text{ij}}^{1M} \\ \vdots & & \vdots \\ Q_{\text{ij}}^{M1} & \cdots & Q_{\text{ij}}^{\text{MM}} \end{bmatrix} \tag{3}$$

where $Q_{\text{ij}}^{\text{uv}}$ is the probability for a node j to retransmit in time slot v a packet that has been transmitted by node i in time slot u. From our network model, it equals to $Q_{\text{ij}}^{uv} = p_{\text{ij}}^u x_{\text{ij}}^{\text{uv}}$.

The arrival matrix $\mathcal{A}$ is given by

$$\mathcal{A} = \begin{bmatrix} \mathcal{A}_{1D_1} & \cdots & \mathcal{A}_{1D_{|\mathcal{D}|}} \\ \vdots & & \vdots \\ \mathcal{A}_{ND_1} & \cdots & \mathcal{A}_{ND_{|\mathcal{D}|}} \end{bmatrix}$$

where $\mathcal{A}_{iD_j}$ is a $|T|$-by-$|T|$ diagonal matrix whose diagonal elements $\mathcal{A}_{iD_j}^u$ give the probabilities for a packet transmitted by a node i in time slot u to arrive at destination D_j and $\mathcal{A}_{iD_j}^u = p_{iD_j}^u$.

Q_S and $\mathcal{A}_S$ are the relaying and arrival matrices for the packets sent by the sources and are given as

$$Q_S = \begin{bmatrix} Q_{S_1 1} & \cdots & Q_{S_1 N} \\ \vdots & & \vdots \\ Q_{S_{|\mathcal{O}|}1} & \cdots & Q_{S_{|\mathcal{O}|}N} \end{bmatrix}$$

and

$$\mathcal{A}_S = \begin{bmatrix} \mathcal{A}_{S_1 D_1} & \cdots & \mathcal{A}_{S_1 D_{|\mathcal{D}|}} \\ \vdots & & \vdots \\ \mathcal{A}_{S_{|\mathcal{O}|}D_1} & \cdots & \mathcal{A}_{S_{|\mathcal{O}|}D_{|\mathcal{D}|}} \end{bmatrix}$$

where $Q_{S_i j}$ follows the pattern given by (3) and $\mathcal{A}_{S_i D_j}$ is a $|T|$-by-$|T|$ diagonal matrix whose diagonal elements are $\mathcal{A}_{S_i D_j}^u = p_{S_i D_j}^u$.

2) Delay Distribution: We assume that one hop introduces a delay of one time unit. Consequently, an h-hop transmission introduces a delay of h units. The delay distribution $P[d_j = h]$ is the probability for a transmission toward D_j to be done in h hops. After s time epochs, a packet can travel up to $h = s + 1$ hops. Thus, the PMF is given by

$$P[d_j = h] = \begin{cases} \frac{\mathcal{A}_S \cdot I_D(D_j)}{f(D_j)} & h = 1 \\ \frac{Q_S \cdot Q^{h-2} \cdot \mathcal{A} \cdot I_D(D_j)}{f(D_j)} & \forall h \geq 2 \end{cases} \tag{4}$$

where $I_D(D_j)$ is a selection vector of dimension $|\mathcal{D}||T|$ where the $|T|$ elements relative to destination D_j are equal to 1 and the others are equal to 0. $I_D(D_j)$ accumulates the packet arrival rate in each time slot at destination D_j. And $f(D_j)$ gives the total packet arrival rate obtained in D_j. This total rate is the sum of the normalized rates obtained from each source sending to D_j : $f(D_j) = \sum_{\forall S_i \in Q_S} f(S_i, D_j)$. The normalized rate provided by source S_i, $f(S_i, D_j)$, is defined in [4] as $f(S_i, D_j) = \sum_{\forall \mathbf{p} \in \mathcal{P}} P(\mathbf{p}) \cdot \tau_{S_i}$, where $\mathcal{P}$ is the set of all possible paths from S_i to D_i, and $P(\mathbf{p})$ is the probability for a packet emitted by S_i to arrive in D_i. This probability is directly obtained from Q and $\mathcal{A}$ matrices.

3) Computing Example for the Delay Distribution: Following, we provide the main derivations that lead to the delay distribution of the 1-flow 3-relay TDMA delay distribution.

For the scenario of interest, there are $|T| = 4$ time slots. The source is transmitting in time slot 1, relay R_1, R_2, and R_3 are transmitting in time slot 2, 3, and 4, respectively. Thus, the relay matrix Q and arrival matrix $\mathcal{A}$ are given as follows (diagonal elements of Q are directly set to 0 since relays do not send data to themselves):

$$Q = \begin{bmatrix} 0 & Q^{23}_{R_1R_2} & Q^{24}_{R_1R_3} \\ Q^{32}_{R_2R_1} & 0 & Q^{34}_{R_2R_3} \\ Q^{42}_{R_3R_1} & Q^{43}_{R_3R_2} & 0 \end{bmatrix}$$

$$= \begin{bmatrix} 0 & p^2_{R_1R_2}x^{23}_{R_1R_2} & p^2_{R_1R_3}x^{24}_{R_1R_3} \\ p^3_{R_2R_1}x^{32}_{R_2R_1} & 0 & p^3_{R_2R_3}x^{34}_{R_2R_3} \\ p^4_{R_3R_1}x^{42}_{R_3R_1} & p^4_{R_3R_2}x^{43}_{R_3R_2} & 0 \end{bmatrix}$$

and

$$\mathcal{A} = \begin{bmatrix} \mathcal{A}^2_{R_1D} & 0 & 0 \\ 0 & \mathcal{A}^3_{R_2D} & 0 \\ 0 & 0 & \mathcal{A}^4_{R_3D} \end{bmatrix} = \begin{bmatrix} p^2_{R_1D} & 0 & 0 \\ 0 & p^3_{R_2D} & 0 \\ 0 & 0 & p^4_{R_3D} \end{bmatrix}.$$

The relaying and arrival matrices Q_S and $\mathcal{A}_S$ for packets sent S are defined as

$$Q_S = \begin{bmatrix} Q^{12}_{SR_1} & Q^{13}_{SR_2} & Q^{14}_{SR_3} \end{bmatrix}$$

and

$$\mathcal{A}_S = \begin{bmatrix} \mathcal{A}^1_{\mathrm{SD}} & 0 & 0 & 0 \end{bmatrix} = \begin{bmatrix} p^1_{\mathrm{SD}} & 0 & 0 & 0 \end{bmatrix}.$$

$I_D(D_j)$ is a dimension selection vector. Since there is only one destination in this example, $I_D(D_j)$ can be denoted by $I_D(D)$. The transpose of $I_D(D)$ is as follows:

$$I^{\mathrm{T}}_D(D) = \begin{bmatrix} 1 & 1 & 1 & 1 \end{bmatrix}$$

$f(D)$ gives the total packet arrival rate obtained in D. For the details of $f(D)$ derivation, we refer the readers to our work in [4]. It is computed as follows:

$$f(D) = \frac{1}{B}[\mathcal{A}^2_{R_1D} \cdot X + \mathcal{A}^3_{R_2D} \cdot Y + \mathcal{A}^4_{R_3D} \cdot Z] + \mathcal{A}^1_{\mathrm{SD}}$$

where

$$\begin{aligned} B = {} & 1 - Q^{23}_{R_1R_2}Q^{34}_{R_2R_3}Q^{42}_{R_3R_1} - Q^{32}_{R_2R_1}Q^{43}_{R_3R_2}Q^{24}_{R_1R_3} \\ & - Q^{34}_{R_2R_3}Q^{43}_{R_3R_2} - Q^{23}_{R_1R_2}Q^{32}_{R_2R_1} - Q^{24}_{R_1R_3}Q^{42}_{R_3R_1} \\ X = {} & Q^{12}_{SR_1}\left(1 - Q^{34}_{R_2R_3}Q^{43}_{R_3R_2}\right) + Q^{13}_{SR_2}\left(Q^{32}_{R_2R_1}\right. \\ & \left. + Q^{34}_{R_2R_3}Q^{42}_{R_3R_1}\right) + Q^{14}_{SR_3}\left(Q^{43}_{R_3R_2}Q^{32}_{R_2R_1} + Q^{42}_{R_3R_1}\right) \\ Y = {} & Q^{12}_{SR_1}\left(Q^{23}_{R_1R_2} + Q^{43}_{R_3R_2}Q^{24}_{R_1R_3}\right) + Q^{13}_{SR_2}\left(1\right. \\ & \left. - Q^{24}_{R_1R_3}Q^{42}_{R_3R_1}\right) + Q^{14}_{SR_3}\left(Q^{42}_{R_3R_1}Q^{23}_{R_1R_2} + Q^{43}_{R_3R_2}\right) \\ Z = {} & Q^{12}_{SR_1}\left(Q^{23}_{R_1R_2}Q^{34}_{R_2R_3} + Q^{24}_{R_1R_3}\right) + Q^{13}_{SR_2}\left(Q^{34}_{R_2R_3}\right. \\ & \left. + Q^{32}_{R_2R_1}Q^{24}_{R_1R_3}\right) + Q^{14}_{SR_3}\left(1 - Q^{23}_{R_1R_2}Q^{32}_{R_2R_1}\right). \end{aligned}$$

The delay distribution $P[d_j = h]$ can be derived by substituting the above matrix in (4).

TABLE II
DCF PARAMETERS FOR DSSS-PHY

PHY	slot σ	SIFS	DIFS	$CW_{\min}$	$CW_{\max}$	m'
DSSS	20 μs	10 μs	50 μs	31	1023	5

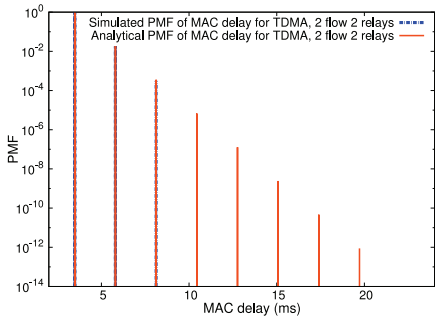

Fig. 4. Analytical and simulated delay PMFs for 2-relay TDMA networks.

IV. RESULTS

First, this section confirms the accuracy of the delay distribution models derived for TDMA and CSMA/CA wireless multihop networks presented earlier by comparing them to fine-grained protocol simulations. Second, the delay distribution and worst-case delay bounds for TDMA and CSMA/CA are compared for the 1-flow and 2-flow topologies illustrated in Fig. 1. Several settings are investigated, mostly related to the TDMA slot duration, the payload size, and the chosen delay–energy tradeoff solution.

A. Simulation Settings

Wireless topologies and protocols are simulated using the realistic discrete event-driven network simulator WSNet.[1] In all topologies, sources only generate frames and destinations only receive them. The sources emit a periodic flow of frames whose period is set differently according to the protocol in use. The end-to-end delay is the duration between the arrival of the frame in the source buffer and the arrival of the frame in destination buffer. Frames have a size of 127 bytes of payload (i.e., the standard maximum IEEE802.15.4 frame size). The data rate is 11 Mbits/s. Simulations are performed for the duration necessary to complete the transmission of 100 000 frames.

1) TDMA Settings: Results are given assuming an additive white Gaussian noise channel and a binary phase shift keying modulation without coding providing a bit error rate of $\mathrm{BER}(\gamma) = Q(\sqrt{2\gamma}) = 0.5 * \mathrm{erfc}(\sqrt{\gamma})$, with γ the per bit signal to noise and interference ratio experienced on the link and erfc the complementary error function. In all topologies, only two nearby nodes communicate with each other (no other node is interfering), they experience a perfect link quality. Moreover, a perfect TDMA is considered, where all nodes are perfectly synchronized. The duration of each time slot is sufficient for

[1] http://wsnet.gforge.inria.fr/

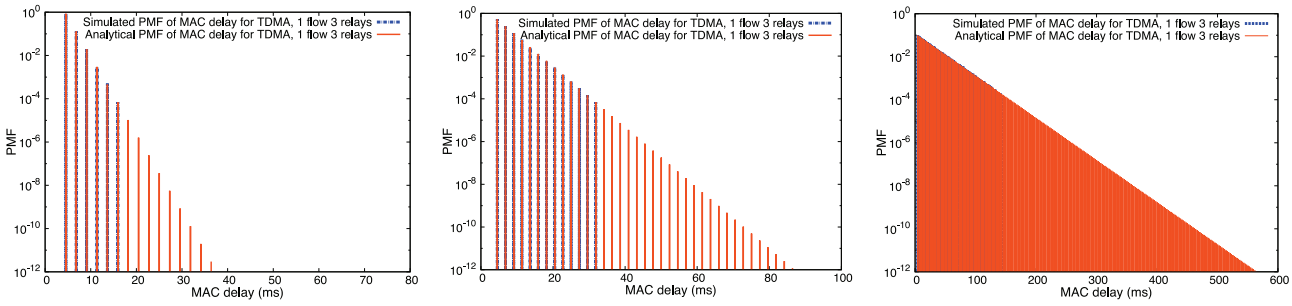

Fig. 5. Analytical and simulated delay PMFs for 3-relay TDMA networks. (a) Delay distribution for $S_{\min}$, (b) delay distribution for S_{middle}, and (c) Delay distribution for $S_{\max}$.

emitting a complete frame. The time slot durations ς_{slot} values are considered here:

a) $\varsigma_{\text{slot}} = 0.29$ ms, the minimum slot duration for sending the frames with 127 bytes of payloads and 24 bytes of the PHY header using IEEE802.11 at 11 Mbits/s.

b) $\varsigma_{\text{slot}} = 10$ ms, the regular slot duration chosen by WirelessHART or ISA100.11a TDMA protocols. Note that both slot durations are long enough to carry a frame with payload of 127 bytes, whether using IEEE802.11 at 11 Mbits/s or IEEE802.15.4 at 250 kbits/s. Relay nodes follow the protocol given in Algorithm 1.

2) CSMA/CA Settings: Presented results for the IEEE802.11 DCF MAC delay are given with the RTS/CTS mechanism. DSSS-PHY layer is assumed. Main DCF timing values are given in Table II. The period of flows emitted by the sources in simulations are derived from the analytical Markov chain model. The analytical Markov chain calculates the end-to-end delay distribution for each flow. From this distribution, it is straightforward to extract the worst-case end-to-end delay. By setting the source periodicity to the worst-case end-to-end delay obtained by the Markov chain model, the simulation reaches the steady state assumed analytically. We have observed in the simulation traces that no packet is kept in his buffer for more than $|T| - 1$ time slots. To be consistent with the Markov model assumptions and fair with TDMA, all nodes of the network have to be in the range of two nodes that are constantly competing for channel access in our simulations.

B. Delay Distribution for TDMA and CSMA/CA Networks

To assess the distance between both analytical and simulated delay distributions, we compute the root-mean-squared error: $\text{RMSE} = \frac{1}{n}\sqrt{\sum_{i=1}^{n} \frac{(d(i)-\tilde{d}(i))^2}{f(i)^2}}$, with n being the total number of points on the graph, and $d(i)$ and $\tilde{d}(i)$ being the analytical and simulated delay values.

1) TDMA Delay Distributions: For the symmetric 2-flow 2-relay topology, the delay distribution for each source–destination pair $S_1 - D_1$ and $S_2 - D_2$ are the same. Delay distribution for TDMA has been computed in this section with the slot duration of 0.29 ms.

As shown in Fig. 4, the analytical delay distribution for one source–destination pair compared with the simulation results for 2-relay TDMA network matches well for most of the delay values that appear the most frequently. The tail of the distribution is very difficult to validate with simulations since such delays are very rare events, with very small probabilities (y-axis of plot is in logscale). However, looking at the overall fit, and the RMSE of $1.7069 * 10^{-3}$ for the computed values, we can conclude that the model seems to be accurate enough (for soft real-time guarantees).

TABLE III
RMSE BETWEEN ANALYTICAL AND SIMULATED DELAY PMF OF TDMA NETWORKS

Scenario	Solution	RMSE
1-flow 3-relay	$S_{\min}$	$3.243 * 10^{-3}$
	S_{middle}	$1.685 * 10^{-3}$
	$S_{\max}$	$3.7659 * 10^{-3}$
1-flow 4-relay	$S_{\min}$	$4.5978 * 10^{-3}$
	S_{middle}	$2.2460 * 10^{-3}$
	$S_{\min}$	$2.7005 * 10^{-3}$
1-flow 5-relay	$S_{\min}$	$7.7249 * 10^{-3}$
	S_{middle}	$1.556 * 10^{-3}$
	$S_{\max}$	$1.734 * 10^{-3}$
2-flow 2-relay	Unique	$3.6301 * 10^{-3}$

We have to stress that the distribution obtained with our TDMA model accounts for all packets received at the destination. As shown in our illustrative example of Fig. 2, packets can travel over the loop (cf., packet P_{10}). In this case, the destination can receive several copies that travelled for a different number of hops in the network. These copies provide redundancy and do explain the tail of the delay distribution calculated here.

For the 3-relay TDMA networks, there are several Pareto solutions, as shown in Fig. 3(b). We recall that we have picked three Pareto optimal solutions to show their delay distribution: $S_{\min}$, S_{middle}, and $S_{\max}$. Their respective distributions are plotted in Fig. 5(a)–(c). The RMSE between analytical and simulated delay PMF for the 2-relay, 3-relay, 4-relay, and 5-relay TDMA networks are given in Table III. Again, these values are really small.

Looking at the impact of the number of relays N on the linear topology, it is interesting to notice that the tail of the $S_{\min}$ delay distribution does not grow much with N. The impact of N is stronger on S_{middle} and $S_{\max}$ distributions. This can

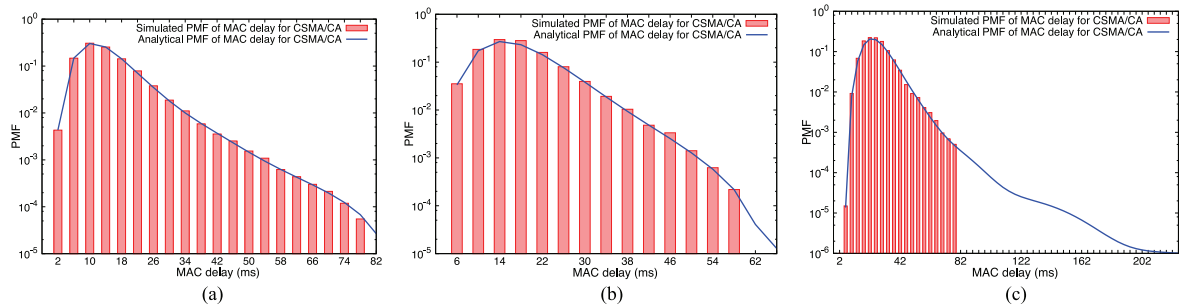

Fig. 6. Analytical and simulated delay PMFs for CSMA/CA networks. (a) Analytical and simulated delay PMFs for 2-relay CSMA/CA network, (b) analytical and simulated delay PMFs for 3-relay CSMA/CA network, and (c) analytical and simulated delay PMFs for 5-relay CSMA/CA network.

TABLE IV
D_W FOR ALL TOPOLOGIES

	δ	D_W for TDMA ($\varsigma_{\text{slot}} = 0.29$ ms)	D_W for TDMA ($\varsigma_{\text{slot}} = 10$ ms)	D_W for CSMA/CA (IEEE802.11 DCF)
2-flow	10^{-5}	10.44 (9 hops)	360	82
2-relay	10^{-6}	12.76 (11 hops)	440	86
	10^{-7}	15.08 (13 hops)	520	88
	10^{-8}	17.4 (15 hops)	600	–
	10^{-9}	19.72 (17 hops)	680	–
1-flow	10^{-5}	20.88 (18 hops)	720	66
3-relay	10^{-6}	23.2 (20 hops)	800	74
	10^{-7}	25.52 (22 hops)	880	78
	10^{-8}	27.84 (24 hops)	960	–
	10^{-9}	30.16 (26 hops)	1040	–
1-flow	10^{-5}	27.55 (19 hops)	950	132
4-relay	10^{-6}	33.35 (23 hops)	1150	188
	10^{-7}	36.25 (25 hops)	1250	316
	10^{-8}	42.05 (29 hops)	1450	428
	10^{-9}	44.95 (31 hops)	1550	1442
1-flow	10^{-5}	34.8 (20 hops)	1200	152
5-relay	10^{-6}	41.76 (24 hops)	1440	314
	10^{-7}	45.24 (26 hops)	1560	676
	10^{-8}	52.2 (30 hops)	1800	1206
	10^{-9}	55.68 (32 hops)	1920	2174

All results are given for $S_{\min}$ solution (Unit: ms).

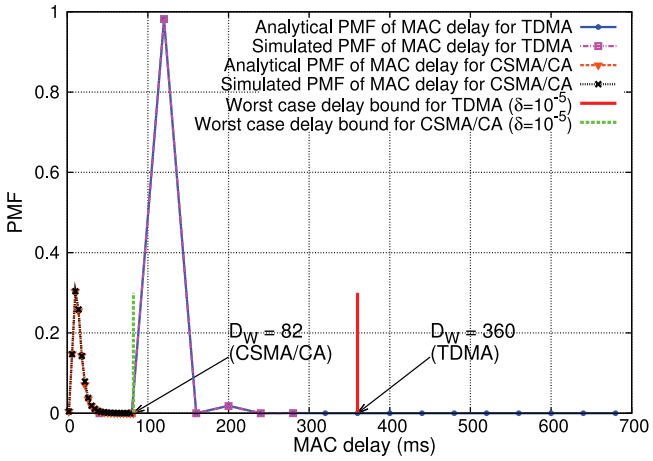

Fig. 7. Worst-case delay bound comparison ($\delta = 10^{-5}$) for 2-relay TDMA and CSMA/CA networks—time slot duration of 10 ms.

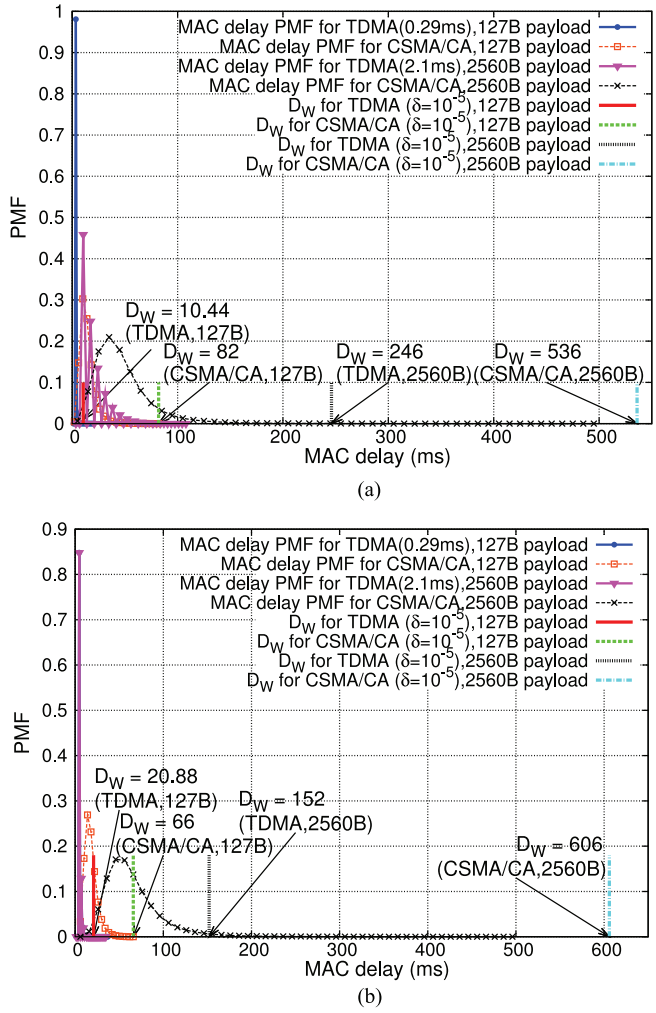

Fig. 8. Worst-case delay bound comparison for different payload sizes for 2-flow 2-relay and 1-flow 3-relay TDMA and CSMA/CA networks. $\delta = 10^{-5}$. (a) 2-flow 2-relay; and (b) 1-flow 3-relay ($S_{\min}$ solution).

be explained by the fact that the loop is rarely used in $S_{\min}$ compared to the two other solutions.

2) CSMA/CA Distributions: We have also verified how good the fit for our CSMA/CA model is. From Fig. 6, we can conclude that analytical and simulated delay distributions match

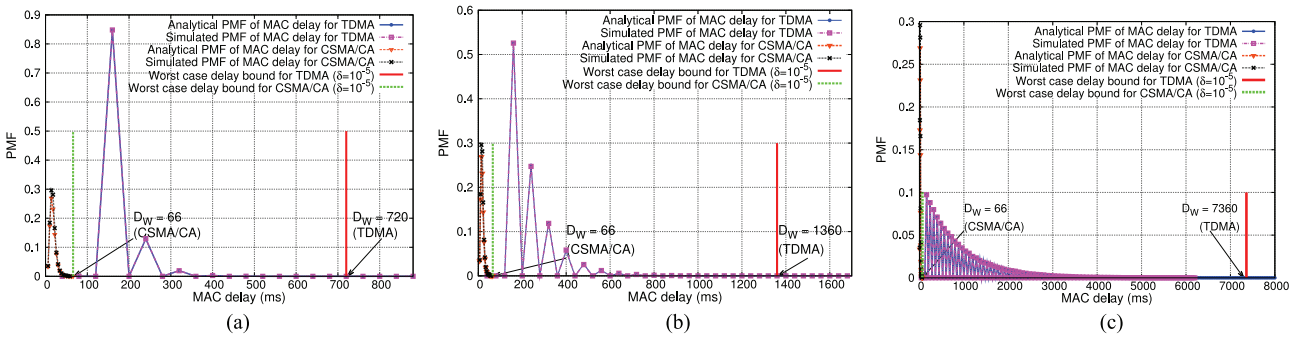

Fig. 9. Worst-case delay bound comparison ($\delta = 10^{-5}$) for 3-relay TDMA and CSMA/CA networks—time slot duration of 10 ms. (a) 3-relay with Pareto optimal solution $S_{\min}$, (b) 3-relay with Pareto optimal solution S_{middle}, and (c) 3-relay with Pareto optimal solution $S_{\max}$.

well, even for the distribution tail of 2- and 3-relays cases. The RMSE is $1.513 * 10^{-2}$ for the 2-relay scenario, $3.213 * 10^{-2}$ for the 3-relay scenario, $3.477 * 10^{-2}$ for the 4-relay scenario, and $3.604 * 10^{-2}$ for the 5-relay scenario.

C. Worst-Case Delay Bound Comparison

TDMA and CSMA/CA worst-case delay bounds have been compared assuming two different time slot duration values. The worst-case delay for 2-relay, 3-relay, 4-relay, and 5-relay topologies are given for different values of δ in Table IV. The comparison of the worst-case delay bounds for 2-relay and 3-relay topologies are illustrated in Figs. 7 and 9.

As shown in Fig. 7, we can see that the worst-case delay bound of TDMA is larger than the one of CSMA for the 2-relay scenario. This plot has been derived for a time slot duration of 10 ms. For a time slot duration of 0.29 ms, however, TDMA is much faster than CSMA/CA, as shown in Table IV. Hence, TDMA can become way more efficient than CSMA/CA by adjusting its time slot duration to a smaller period. But, in practice, larger slots are chosen to mitigate the impact of synchronization errors, at the cost of overall performance degradation, as shown here. However, the tail of the TDMA distribution is much shorter than the one of CSMA. Thus, TDMA systems exhibit a slower increase in d^w as accuracy increases (and δ reduces).

For the 3-relay CSMA/CA network, the worst-case delay bound with $\delta = 10^{-5}$ is of 66 ms. As shown in Fig. 9(a), d^w of TDMA obtained with $S_{\min}$ and a 10 ms slot is still larger than the worst-case delay of CSMA/CA. But for the time slot duration of 0.29 ms, TDMA is faster than CSMA/CA. Note that we have not accounted for the synchronization overhead in our TDMA derivations.

D. Worst-Case Delay Bound for Different Payloads

In this section, we compare the worst-case delay bound for different payload sizes. Fig. 8(a) and (b) illustrate the results for the 2-flow 2-relay topology and the 1-flow 3-relay topology, respectively. All previous results were given for a payload size of 127 bytes. Here, we investigate the impact of payload by comparing the distributions obtained for TDMA and CSMA/CA with a 127 bytes payload to a 2560 bytes payload (i.e., the maximum frame size of IEEE802.11). This extended payload is modeled in TDMA by setting ς_{slot} to 2.1 ms. Not surprisingly, the smaller the payload, the smaller the worst-case delay bound. Even for of 2560 bytes (which is unusual for wireless sensor networks), TDMA performs better than CSMA/CA. This clearly calls for 1) implementing microsecond or submicro-second level synchronization algorithms to reduce the TDMA slot size from 10 ms slots to 3 ms slots, and 2) introducing the overhead introduced by such an algorithm in the delay distribution derivations.

V. Related Works and Discussion

Currently, only few works have addressed the problem of worst-case delay bound calculation for wireless multihop networks. They have focused on deriving either a deterministic or a probabilistic bound. Deterministic bound calculation methods encompass two pieces of works. The first piece is based on network calculus and has been proposed by Schmitt and Roedig [11] and extended in their later works to include the processing resources on the sensors. The analytical model is named *Sensor Network Calculus*. In [12] and [13], it has been applied to analyze the IEEE802.15.4 cluster-tree WSNs. In the aforementioned works, it has been assumed that transmissions follow a perfect TDMA. Thus, the service curve can be approximated by a rate–latency curve. Assuming that the channel is perfect during the specified time window may be too optimistic in some cases. Localized interference may lead to a sudden drop in signal to noise ratio, triggering additional delay before perfect reception. Moreover, additional to such an analysis, it is necessary to measure the quality of the synchronization protocol used to ensure this perfect TDMA. There is a risk with such an approach to underestimate the worst-case delay bound. In other words, network calculus provides a purely deterministic analytical framework, which may be too rigid to capture the probabilistic nature of wireless transmissions. Moreover, it is not straightforward to capture the delay performance of contention-based medium access protocols such as CSMA with network calculus.

The later works for deterministic bound calculation rely on model checking [14], [15]. These papers can only address small scale networks since for a simple five-node sensor network cluster, enumerating all possible topologies needs more than 8000 model checking runs. Despite the small number of nodes, this approach gave valuable insight into the protocol and the scenarios that lead to collisions not being detected by the protocol. To better capture the link error probabilities, it is proposed in [15] to calculate in parallel the probability for the

considered property to be verified knowing the probability that a given topology exists due to possible link packet error rates. But still, the well-known combinatorial explosion pitfall of model checking seems to be the main obstacle for a successful validation for real-time networks. Such networks carry more than a thousand real-time multicast flows, thus, deriving a scalable method is essential. Models of this paper are way more scalable as their complexity grows only with the number of nodes, and not with the number of flows carried in the network. Indeed, the matrix representation we leverage in our TDMA model and the Markov chain calculations for CSMA/CA can handle several source flows with the same complexity, provided that the number of nodes is not changed.

More recent works look at the problem from a probabilistic point of view, defining the worst-case end-to-end delay d^w, as in this paper. In this vein, probabilistic network calculus has been applied in [16] to provide a quality of service aware method that captures wireless fading channels. Probabilistic network calculus leverages moment generating functions. The study exploits a service curve for a Gilbert–Elliott channel with memory representative of a realistic fading channel. Results show clearly that the fading speed of the wireless medium impacts the service guaranties significantly.

A closely related work is the one of Despaux *et al.* [17], which leverages the probabilistic framework of reliability calculus proposed in [18]. Reliability calculus relies on a stochastic model of the network where links are modeled using a packet error rate, and nodes with a probabilistic decision to forward a received message on a given link. Using the Laplace transform, He *et al.* [18] manage to calculate the delay distribution of flows in a multihop network. Despaux *et al.* [17] have leveraged this stochastic model to calculate the delay performance of the ContikiMAC protocol. Therefore, they use process-mining techniques to abstract the protocol process into a Markov chain to feed the model mentioned in [18]. This abstraction is essential to capture the behavior of the protocol from very long execution traces. These execution traces encompass the behavior of the MAC protocol, but also the impact of the wireless channel at the time of recording. The network model of reliability calculus is close to the one proposed in our work, but our approach is more general: It can be leveraged to calculate a wide variety of network metrics that can be used to optimize networking decision (i.e., forwarding probabilities).

VI. Conclusion

This paper provides an overview of two models whose aim is to calculate the worst-case delay bounds d^w for TDMA and CSMA/CA-based wireless multihop networks. An original contribution of this work is the analytical delay distribution model for TDMA. After calculating the d^w bounds for TDMA and CSMA/CA for both topologies, we have investigated the impact of the TDMA slot duration and payload on d^w. We can show that this choice clearly impacts the worst-case bound performance of TDMA, as expected. In future works, we plan to validate our model against real experiments. It will be interesting as well to be able to control the load pushed into the network to capture its impact on both multiple access methods.

References

[1] S. Zhuo, Z. Wang, Y. Q. Song, Z. Wang, and L. Almeida, "iQueue-MAC: A traffic adaptive duty-cycled MAC protocol with dynamic slot allocation," in *Proc. 10th Annu. IEEE Commun. Soc. Conf. Sensor, Mesh Ad Hoc Commun. Netw.*, Jun. 2013, pp. 95–103.

[2] S. Petersen and S. Carlsen, "WirelessHART versus ISA100.11a: The format war hits the factory floor," *IEEE Ind. Electron. Mag.*, vol. 5, no. 4, pp. 23–34, Dec. 2011.

[3] P. Suriyachai, U. Roedig, and A. Scott, "A survey of MAC protocols for mission-critical applications in wireless sensor networks," *IEEE Commun. Surveys Tuts.*, vol. 14, no. 2, pp. 240–264, Second Quarter 2012.

[4] Q. Wang, K. Jaffrès-Runser, C. Goursaud, J. Li, Y. Sun, and J.-M. Gorce, "Deriving pareto-optimal performance bounds for 1 and 2-relay wireless networks," in *Proc. IEEE Int. Conf. Comput. Commun. Netw.*, Nassau, Bahamas, Aug. 2013, pp. 1–7.

[5] Q. Wang *et al.*"A thorough analysis of the performance of delay distribution models for IEEE 802.11 DCF," *Ad Hoc Netw. J.*, vol. 24, pp. 21–33, 2015.

[6] L. Pinto, A. Moreira, L. Almeida, and A. Rowe, "Aerial multi-hop network characterization using cots multi-rotors," in *Proc. IEEE World Conf. Factory Commun. Syst.*, May 2016, pp. 1–4.

[7] J. Vardakas, M. K. Sidiropoulos, and M. Logothetis, "Performance behaviour of IEEE 802.11 distributed coordination function," *IET Circuits, Devices Syst.*, vol. 2, no. 1, pp. 50–59, 2008.

[8] H. Zhai, Y. Kwon, and Y. Fang, "Performance analysis of IEEE 802.11 MAC protocols in wireless LANs," *Wireless Commun. Mobile Comput.*, vol. 4, no. 8, pp. 917–931, 2004.

[9] G. Bianchi, "Performance analysis of the IEEE 802.11 distributed coordination function," *IEEE J. Sel. Areas Commun.*, vol. 18, no. 3, pp. 535–547, Sep. 2000.

[10] H. Vu and T. Sakurai, "Accurate delay distribution for IEEE 802.11 DCF," *IEEE Commun. Lett.*, vol. 10, no. 4, pp. 317–319, Apr. 2006.

[11] J. B. Schmitt and U. Roedig, "Sensor network calculus—A framework for worst case analysis," in *Proc. 1st IEEE Int. Conf. Distrib. Comput. Sensor Syst.*, 2005, pp. 141–154.

[12] A. Koubaa, M. Alves, and E. Tovar, "Modeling and worst-case dimensioning of cluster-tree wireless sensor networks," in *Proc. 27th IEEE Int. Real-Time Syst. Symp.*, Dec. 2006, pp. 412–421.

[13] L. Lenzini, L. Martorini, E. Mingozzi, and G. Stea, "Tight end-to-end per-flow delay bounds in fifo multiplexing sink-tree networks," *Perform. Eval.*, vol. 63, no. 9, pp. 956–987, Oct. 2006.

[14] A. Fehnker, L. Van Hoesel, and A. Mader, "Modelling and verification of the LMAC protocol for wireless sensor networks," in *Proc. 6th Int. Conf. Integr. Formal Methods*, 2007, pp. 253–272.

[15] A. Mouradian and I. A. Blum, "Formal verification of real-time wireless sensor networks protocols: Scaling up," in *Proc. 26th Euromicro Conf. Real-Time Syst.*, Jul. 2014, pp. 41–50.

[16] M. Fidler, "Wlc15–2: A network calculus approach to probabilistic quality of service analysis of fading channels," in *Proc. IEEE Global Telecommun. Conf.*, Nov. 2006, pp. 1–6.

[17] F. Despaux, Y. Q. Song, and A. Lahmadi, "Modelling and performance analysis of wireless sensor networks using process mining techniques: Contikimac use case," in *Proc. IEEE Int. Conf. Distrib. Comput. Sensor System*, May 2014, pp. 225–232.

[18] W. He, X. Liu, L. Zheng, and H. Yang, "Reliability calculus: A theoretical framework to analyze communication reliability," in *Proc. IEEE 30th Int. Conf. Distrib. Comput. Syst.*, Jun. 2010, pp. 159–168.

Qi Wang received the Ph.D. degree in computer science from the Chinese Academy of Sciences, Beijing, China, in 2015.

In 2010, she received a one-year fellowship from INRIA to pursue her research within the SWING team of INRIA and INSA Lyon. She visited the University of Toulouse in 2012 thanks to the 2012 EIFFEL doctoral fellowship from the French Ministry of Foreign Affairs. She is currently an Assistant Professor in the Institute of Computing Technology, Chinese Academy of Sciences, Beijing, China. Her research interest includes the performance evaluation of wireless networks for delay sensitive applications.

Katia Jaffrès-Runser (M'05) received the Dipl.Ing. and M.Sc. degree in 2002, and the Ph.D. degree in computer science from INSA Lyon, Villeurbanne, France, in 2005.

From 2002 to 2005, she was with Inria. In 2006, she joined the Stevens Institute of Technology as a Postdoctoral Researcher. She has been an Associate Professor with the University of Toulouse, Toulouse, France, since 2011. She received a three-year Marie-Curie OIF fellowship from the European Union (2007–2010). Her research interest include the performance evaluation of wireless networks in general, with a special focus on real-time guaranties provision.

Yongjun Xu (M'03) received the B.Eng. degree from Xi'an Institute of Posts & Telecoms, Xi'an, China, in 2001 and the Ph.D. degree from the Institute of Computing Technology, Chinese Academy of Sciences (ICT-CAS), Beijing, China in 2006, both in computer communication.

He is currently a Professor in the ICT-CAS. His current research interests include wireless sensor network, cyber-physical systems and multisensor data fusion.

Jean-Luc Scharbarg received the Ph.D. degree in computer science from the University of Rennes, Rennes, France, in 1990.

He has been an Associate Professor in the Université de Toulouse (INPT/ENSEEIHT and IRIT Laboratory) since 2002, where he has also been a Full Professor since 2012. His current research interest include the analysis and performance evaluation of embedded networks, mainly in the context of avionics and automotive.

Zhulin An received the B.Eng. and M.Eng. degrees in computer science from the School of Computer and Information, Hefei University of Technology, Hefei, China, in 2003 and 2006, respectively, and the Ph.D. degree in computer science from the Institute of Computing Technology, Chinese Academy of Sciences (ICT-CAS), Beijing, China, in 2010.

He is currently an Associate Professor in the ICT-CAS. His research interests include parallel and distributed system and time synchronization in wireless network.

Christian Fraboul received the Engineering degree from INPT/ENSEEIHT, Toulouse, France, in 1974.

From 1974 to 1998, he was a Research Engineer at ONERA. Since 1998, he has been a Full-Time Professor at INPT, where he led the Department of Telecommunications and Networks, ENSEEIHT, and the IRT team of the IRIT Laboratory. His main research interests include embedded networks architectures and performance evaluation of such architectures (mainly in avionics context).